

Process Variability in Micro-Embossing

David Hardt, Bala Ganesan, Matthew Dirckx, Grant Shoji, Kunal Thaker and Wang Qi

Laboratory for Manufacturing and Productivity

Massachusetts Institute of Technology

Singapore MIT Alliance Programme in Innovation in Manufacturing Systems and Technology

Abstract— A promising technique for the large-scale manufacture of micro-fluidic devices and photonic devices is hot embossing of polymers such as PMMA. Micro-embossing is a deformation process where the workpiece material is heated to permit easier material flow and then forced over a planar patterned tool. While there has been considerable attention paid to process feasibility very little effort has been put into production issues such as process capability and eventual process control. In this paper, we present initial studies aimed at identifying the origins and magnitude of variability for embossing features at the micron scale in PMMA. Test parts with features ranging from 3.5- 630 μm wide and 0.9 μm deep were formed. Measurements at this scale proved very difficult, and only atomic force microscopy was able to provide resolution sufficient to identify process variations. It was found that standard deviations of widths at the 3-4 μm scale were on the order of 0.5 μm leading to a coefficient of variation as high as 13%. Clearly, the transition from test to manufacturing for this process will require understanding the causes of this variation and devising control methods to minimize its magnitude over all types of parts.

Index Terms

Microembossing, PMMA. Variability, Process Control

I. INTRODUCTION

THE process of embossing thermoplastic materials is not a new one, but it is receiving renewed attention as a good candidate for high volume production of micro-fluidic and micro-optical devices. It is a single step process for net-shape forming of components that might otherwise require multiple processing steps using conventional lithographic processes on glass or semiconductor substrates. One of the key materials for such products, polymethylmethacrylate (PMMA) has both good processing characteristics and good functional characteristics. In the latter, it is favored for both optical clarity and fluid compatibility.

Given the goal of using micro-embossing for high volume

production of such devices, it is imperative that the ultimate process capability be established early on to help product designers understand the dimensional precision limits imposed by this choice. This work is a first step in developing a fundamental understanding of process variability, the causal factors, and the possible process design and control changes that can be made to improve the precision limits.

II. TARGET APPLICATIONS AND PROCESSES REQUIREMENTS

There is considerable literature regarding the use of embossed components in micro devices, and they tend to fall into the following broad categories:

- Micro reactors e.g. [1, 2]
- Micro fluidic flow systems for physical separation [3, 4]
- Micro optical devices [5, 6]

In all cases the product performance depends upon creating patterns or features in a polymer workpiece that have characteristic dimensions in the 0.1 to 100 μm range. There is currently a move to net shape forming (e.g. embossing and injection molding) of polymers for applications in the biomedical field. As pointed out in [7] and [8], this is motivated by the prospect of high production rates and lower costs when compared to the traditional methods using glass or silicon and lithography based methods. The attributes of embossing are particularly relevant in the biomedical field, where disposability is important and the customer base large and repetitive. In addition, many polymers (such as PMMA) have good biocompatibility and favorable optical properties. As a result, there have been many recent publications looking at the use of embossed components in the above application area.

Since many of these devices work with picoliters of fluids, and often with fluids carrying large molecules or cells, certainty in the fluid mechanics of the devices is imperative to robust device performance. In addition, the smallest dimensions in use in this field (typically 10 μm and larger channels) have not yet approached the limits of ~ 25 nm demonstrated by Chou et al. [9]. Thus, it is clear that the ultimate limits of devices in terms of size, performance robustness production speed and costs will depend on knowledge of the limits of the dimensional variation (i.e. precision) that this process can provide.

D.E. Hardt is Professor of Mechanical Engineering at MIT and MIT Co-Chair of the Singapore MIT Alliance Programme Innovation in Manufacturing Systems and Technology (hardt@mit.edu)

B. Ganesan (Ganesan@alum.mit.edu) is now with McKinsey & Company, Orange County, CA. M. Dirckx (mdirckx@mit.edu), G. Shoji(gshoji@mit.edu), K. Thacker (thakerkh@mit.edu) and Q. Wang (wqi@mit.edu) are research assistants in the Laboratory for Manufacturing and Productivity at MIT.

III. PROCESS QUALITY ASSESSMENT

While there has been much research on the basic feasibility of micro-embossing, very little work has focused on the quality of the final product. (See [10] for a review of this topic.) Since the overall goal of process control is to regulate quality of the final product, it is vital to know the key characteristics and problems with these that can arise during the embossing process. The work of Roos *et al.* [11] is significant in that it establishes a measurable set of attributes that can be used for statistical studies, process optimization and ultimately for active process control. By looking at features such as “LISA” defects (self assembled trenches at the surface), viscous fingering and degree of filling, they were able to distinguish the performance of various processing regimes. In a related paper, Roos *et al.* [12] investigated the use of a commercial embossing system, for making PMMA parts with features ranging from 0.4 to 100 μm on a large-scale (4in) workpiece. They also assessed quality based on the degree of filling (as opposed to specific dimensional variation). They identify temperature and hold time as critical to forming success, and imply that pressure needs to be above a certain threshold, but is the least sensitive variable of the three. Unfortunately, the quality assessment is rather qualitative, and serves only to support the conclusion that such multi-scale forming over a large area is feasible.

Specific statistical data for micro-embossing is presented in Lee *et al.* [13] who are interested in bio-fluidic applications. Since they seek an inexpensive, disposable product, their concern is inherently related to true manufacturing, and accordingly, to process statistics over a large ensemble of products. They fabricated a number of identical devices with identical processing conditions to look for variation in specific dimensions, rather than more binary “defects”. For example, they noted that over 10 separate parts, the surface profiles (including 100mm width channels 400 μm deep) had an average width of 102.9 μm and a relative standard deviation of 2.2%. This implies an absolute standard deviation of 2.3 μm . The relative depth standard deviation was quoted as “less than 1%” on an average of 39.12 μm . They also characterized their etched quartz tool and concluded that reproduction is very good with micro-embossing. However, the dependence of these statistics on processing conditions (rate, temperature, pressure) was not investigated.

Bacon *et al.* [14] describe a series of embossing experiments with 300 – 500 μm features in PMMA. Using fixed hold time and no vacuum, they varied the embossing force and the temperature of the top and bottom forming platens from ambient to $> T_g$. An output data table is presented for a total of 21 different combinations of these inputs and the outputs are listed in terms of relative quality of pattern reproduction (similar to Roos *et al.* [11]). While only a start, this work is an example of the basic empirical characterization of embossing that can be done using some form of designed experiments. However, there was no attempt to determine a specific functional relationship between input settings and output quality.

In a paper that directly addresses the issue of “manufactur-

ing environment”, Lin *et al.* [15] compare the quality of devices made in a laboratory environment with those made in a commercial environment. In both cases they were concerned with forming 30 μm micro-pyramids. The lab process used PMMA while the commercial process used PVC. There was no attempt to tune the processes, and the main distinction (aside from the material) was the processing time. The lab process, given a total cycle time of 2 hours was able to reproduce the tool faithfully, while the commercial process, operating on a 1 minute cycle time, did not.

Finally, in Lin *et al.* [16], the problem of quality is addressed from a fundamental point of view, with an analytical and simulation study of shrinkage in hot micro-embossing of PMMA. While there is no empirical verification of the results, they do conclude that proper use of holding pressures during cooling can greatly reduce the amount of shrinkage, similar to common practice in injection molding.

IV. THE MICRO-EMBOSSING PROCESS

The process of hot embossing of thermoplastic polymers involves the plastic flow of material around a tool that has a shape inverse of the desired part shape. The material is first heated to a point between the glass transition temperature (T_g) and the melting temperature (T_i) and then the tool is pressed into the material uniaxially. (It is the polymeric equivalent of a hot forging process.) This sequence is shown schematically in Fig. 1.

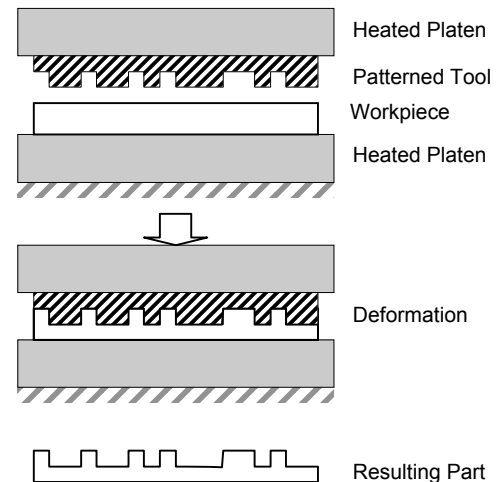


Figure 1 Basic Steps in Embossing

The process proceeds by first heating the material and tool and then applying a forming force. As this force is applied, the material begins to flow into the tool, initially flowing across the boundary of the tool features. Once complete filling of the features has occurred, the forming pressure is held for a sufficient time to allow for the visco-elastic material to flow into the tool. This hold time is a function of both material temperature and forming force. A typical time history of these variables is shown schematically in Fig. 2.

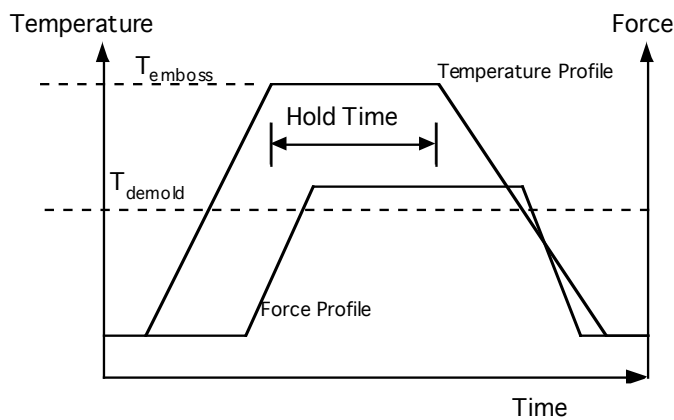


Figure 2 Typical Forming Cycle for Temperature and Force

V. FORMING APPARATUS

A lab scale machine was developed to execute preliminary experiments in micro-embossing. Although commercial micro embossing machines are available, a decision was made to fabricate the experimental apparatus to allow better understanding of the process dynamics and to have the flexibility of designing its control system. The apparatus is designed to be capable of producing a single part per machine cycle. To meet these needs, a commercial material testing machine, an Instron Model 5869 was chosen. A corresponding lab-scale set up for embossing is shown in Fig. 3. This setup includes heated platens, tool and workpiece holders, and a single axis actuator for applying a well controlled forming forces. (Details of the design and performance of this machine can be found in [17]).

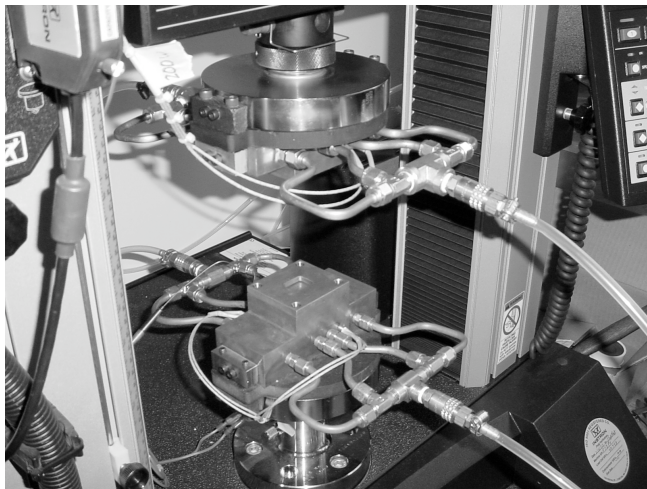


Figure 3 A Lab-Scale Embossing Setup at MIT

The success of this process is measured both by the dimensional accuracy of the final part and the presence of residual stresses that may affect performance. Depending on the application, both feature dimensions and surface finish will be of concern.

The Instron 5869 is a table mounted materials testing system of capacity 50KN (11250lb) and has a test speed range of 1 μ m/min to 500mm/min (0.00004in/min to 20in/min) with a 50KN load cell. It can deliver a load accuracy of +/- 0.4N and

position control accuracy of 0.063 μ m. The 5869 provides closed loop control of force or displacements of the platens with control algorithms written in LabVIEW allowing the flexibility of programming specific trajectories.

A. Platens

The platens are one of the most critical components of the hot embossing machine. The platens hold and maintain the orientation of the work piece and the tool, supply and evenly distribute heat, as well as cool the work piece and tool, and maintain structural rigidity while load is imposed on the work piece during the embossing process.

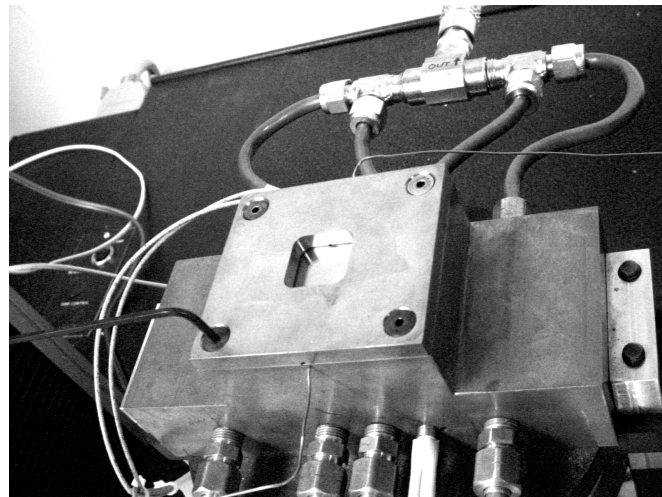


Figure 4 Copper Lower Platen. Notice the workpiece holder, the cooling water tubing and the wires leading to the cartridge heaters.

The platens used in this work were fabricated from copper owing to its superior heat diffusivity and sufficient strength. (See Fig. 4). They are heated with 2 – 200 W cartridge heaters, and temperature control was implemented with a thermocouple sensor and a commercial PI temperature controller (Chromolox 2110). The dimensions of the copper and the location of the heaters was chosen to insure a uniform temperature at the forming surfaces. However, the large mass of copper required more than 10 minutes to raise the temperature to the forming temperature of 150 $^{\circ}$ C. Cooling was provided by city water introduced through 4 – 6.5 mm diameter passages at full pressure. This was capable of cooling the assembly from 150 to 50 $^{\circ}$ C in 5 minutes.

B. Tooling

A silicon tool used for the experiments was produced by etching features of constant depth using DRIE. The tool has 3 different groups of features etched to an average uniform depth of 0.9 microns. The first group of features is the letters “MIT” and “TIM” etched symmetrically at different scales (See Fig. 5). The features “MIT” and “TIM” will be referred to as the left and right “MIT” features respectively from now onwards. The letters are etched at six different scales with each scale being approximately double the size of its directly smaller scaled feature. The smallest letter is 3.5 microns wide

(width of a vertical portion of a letter “I”). These features create raised letters on the PMMA part once embossed. For the purpose of reference in this thesis, the biggest scale is named as “Scale 1” and the smallest scale as “Scale 6” (see Figure 5).

The second group of features is a set of trenches of various widths but of the same length and depth. These trenches are all about 900nm deep and create plateau-like raised features on the PMMA part when embossed. The third group of features is a set of squares. These squares are present at different scales and similarly create raised features on the PMMA part.

The tool used for the experiments produces a number of features that could be studied, but to restrict the scope of this project, only the group of features with the “MIT” letters was chosen for study as this group of features had the most variety of features with different aspect ratios and intricate shapes, adding more feature variety.

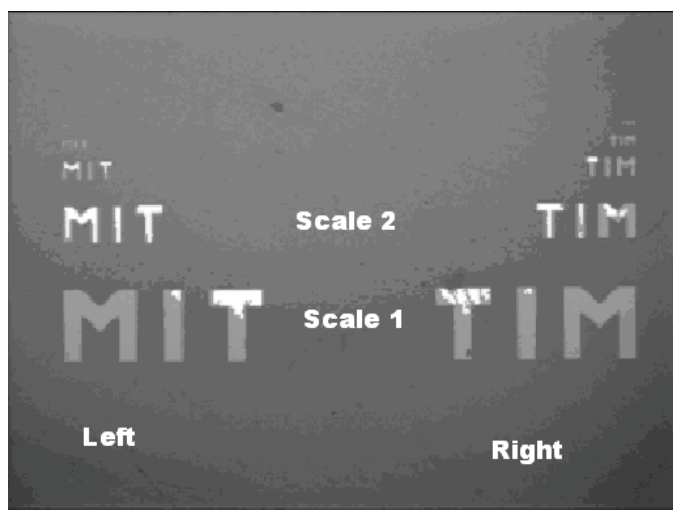


Figure 5 Typical Tooling Features. These feature range in width accruing to table 2, and are all of 0.9 μm depth.

VI. EXPERIMENTAL METHODS

The temperatures for both top and bottom platens were kept at 135°C for all the experiments, which is 30°C above the glass, transition temperature of PMMA. When lower platen temperatures of about 120°C were used during preliminary trials, the parts were seen to partially fill and craze marks were evident. The tool was given two displacement rates: a fast rate as it approaches the PMMA, and a slower rate after 10N of force is detected. A typical displacement history is shown in Figure 6. The displacement rate before contact was kept at 2mm/min and the forming rate was reduced to 0.075mm/min. The maximum embossing force was kept at 90N and once this force is reached, the tool position is kept constant for 240 seconds. After that, the platens are cooled at a rate of -1.30°C/sec until the temperature of the bottom platen is 60°C. At this point, the load is released and the part de-molded. The hold time of 240 seconds was also determined through pre-experimental trials. Hold times of less than 120 seconds yields parts with features not embossed fully and hold time of 240 seconds was found to be sufficient for this experimental setup.

The specific values used are shown in Table 1

Control Inputs	Values
Maximum Temperature (Top platen)	135°C
Maximum Temperature (Bottom platen)	135°C
Before Contact Rate	2mm/min
Contact Trigger force	10N
After Contact Rate	0.075mm/min
Maximum Force	90N
Hold Time	240Sec
Cooling Rate	-1.3°C/sec
De-mold Temp	60°C

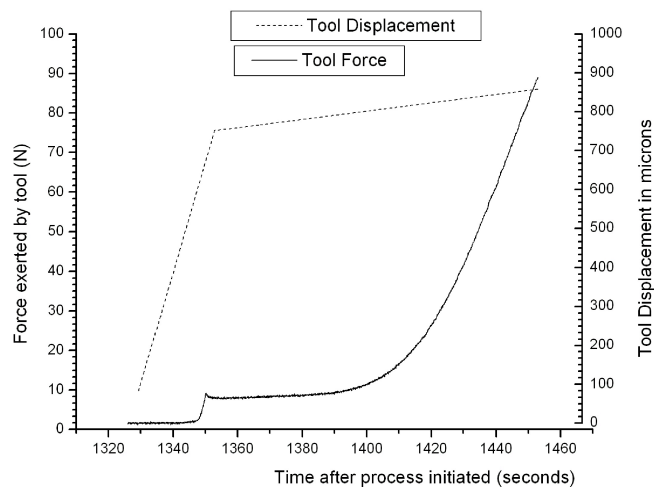


Fig 6 Temperature and Force control plot for a typical embossing process

VII. EXPERIMENT OBJECTIVES

The objective here is to produce a number of identical parts and then compare critical dimensions on successive parts. In this way, the variation of the process can be quantified. In addition, by looking at features of different size and location on the tool, potential sources of variation can be identified.

To examine the extent of dimensional variations with a fixed set of control inputs, 10 replicates were conducted using the conditions in Table 1. For each location shown on Fig. 7 a width measurement is made and thus run charts for the 10 replicates can be produced. From these we can determine basic process variability, and by comparing these statistics over the various part features we can examine the effect of feature size, location and shape.

VIII. MEASUREMENTS

The width of various features on the part was chosen as the key characteristic for measurement, owing to each of location and its ultimate role in determining micro-fluid flow channels cross section. The features chosen are shown in Fig. 7. The same features were measured on all size scales except the

smallest.

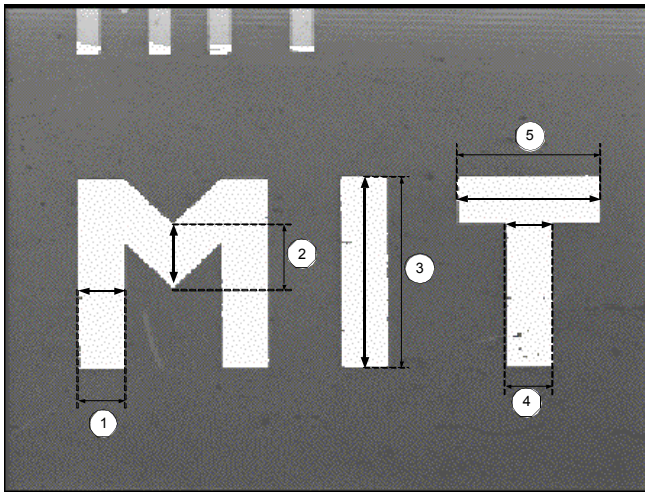


Figure 7 – Part features chosen for measurement

The different scales of features will be identified by the leg width “4” on each as shown in Table 2.

TABLE 2
NOMINAL WIDTH DIMENSIONS FOR THE SIX MIT FEATURES

Scale	Dimension # 4 (microns)
1	170
2	89
3	44
4	24
5	13
6	4

IX. MEASUREMENT METHODS

The parts were initially measured using a Zygo model 5000 series optical profilometer. This device has a vertical measurement resolution of 0.1nm, but as a much larger horizontal resolution, depending on the desired field of view. The measurement is based on scanning white-light interferometry, a traditional technique in which a pattern of bright and dark lines (fringes) results from an optical path difference between a reference and a sample beam. Incoming light is split inside an interferometer, one beam going to an internal reference surface and the other to your sample. After reflection, the beams recombine inside the interferometer, undergoing constructive and destructive interference and producing the light and dark fringe pattern.

A. Limitations of Optical Interferometry

The optical profilometer posed some problems in measuring the smaller “MIT” features since the transparent PMMA, makes focusing the interference fringe patterns difficult. As a result, the smallest set of “MIT” features (Scale 6) were not used for the analysis. More importantly, the maximum horizontal resolution attainable varied with feature scale, as shown in Table 3. This limitation is inherent in any optical device

where a fixed measurement resolution is spread over a variable field of view.

TABLE 3
RESOLUTION – RANGE RELATIONSHIP FOR THE ZYGO INTERFEROMETER

Scale	Horizontal Resolution (microns)	Nominal Width (microns)
1	2.2	170
2	2.2	89
3	0.85	44
4	0.85	24
5	0.85	13
6	N/A	4

Another difficulty was presented by the shape of the tool and the resulting part. The Deep Reactive Ion Etching (DRIE) process leaves sidewalls with a distinct draft angle and such, the respective top and bottom feature dimensions of the tool, as well as the embossed parts, are different. Accordingly, for all subsequent measurements reported here, the top width of the features is used.

B. Limited Resolution Effects

On all ten features shown in Fig. 5 width data was collected and first plotted in a series of run charts. A typical chart for Scale 1 is shown in Fig. 8. At first, it appears that the data is typical of a production process in a state of statistical control, as there are no obvious trends or other deterministic behavior. Indeed a test of the data indicated it is well modeled by a normal probability distribution.

However, it is important to note that the degree of variations (~ 2 microns) evident in this plot is the same magnitude as the horizontal measurement resolution of the interferometer. This is emphasized by the $\pm 1.1 \mu\text{m}$ error bars on the plot. This implies that the variation observed could just as well be attributed to the measurement as to the production process. Unfortunately, this same trend continued even at the lower scales.

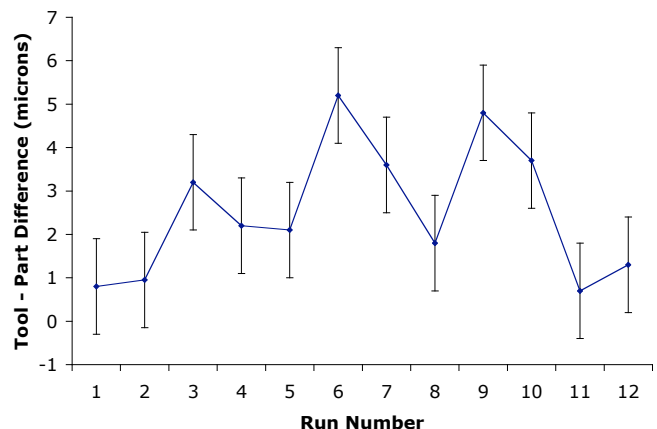


Figure 8 A Run Chart of Feature 1 Scale 1 Dimensions with resolution error bars included. (NB: The actual tool – part difference is plotted, not the absolute part dimension.)

As further evidence of the influence of the limited resolution, consider Figure 9. Here the standard deviation of all parts formed for all different scales is collected to see if there existed a relationship between scale and magnitude of deviations. As can be seen there appears to be a strong relationship, with larger features leading to larger deviations. However, if one superimposes the resolution data from Table 3 on this plot, it nearly matches the magnitude of the deviation, again casting doubt on whether the observation of measurement or process variation.

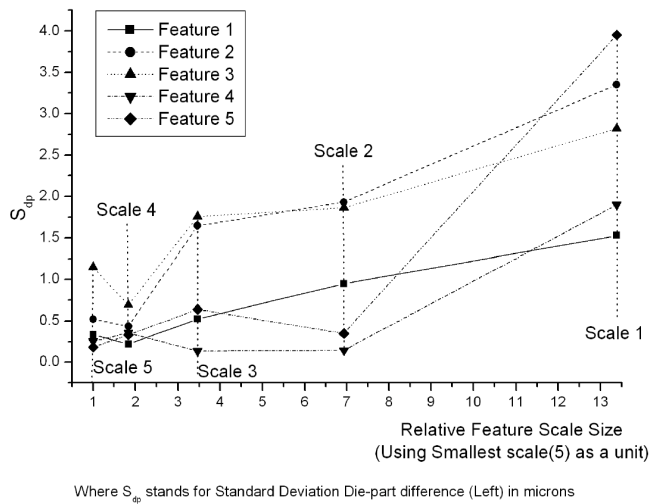


Figure 9 Standard Deviation of Tool-Part Difference for All Features and All Scales.

C. Atomic Force Microscopy

To resolve the ambiguity between variation in the measurement method and the process itself, a method of higher horizontal resolution was needed. The limitations inherent in optical profilometry suggest an alternative, and atomic force microscopy (AFM) was chosen. Using a Quesant Q-Scope Model 250 the horizontal resolution of the scans taken was approximately 60 nm. These scans could produce images of a scale 6 (~4 micron) feature such as shown in Fig. 10. As a check on the validity of the detailed surface data from the AFM, environmental-SEM pictures were also taken using a Philips/ FEI XL30 FEG-SEM. The comparison between ESEM and AFM is excellent, leading to the conclusion that variation seen in the AFM data is dominated by the part and not the measurement.

Using the AFM in contact mode, the parts were measured by direct surface profiling, so measurement resolution was limited only by the scanning resolution of the device. A typical measurement for the 'I' feature width is shown in Fig. 11. Although higher resolution than optical techniques, the AFM produces artifacts in certain locations along the scanning direction, therefore the most accurately produced features were observed to be perpendicular to the scanning direction. The features used to determine process variation were oriented perpendicular to the scanning direction to ensure controller related

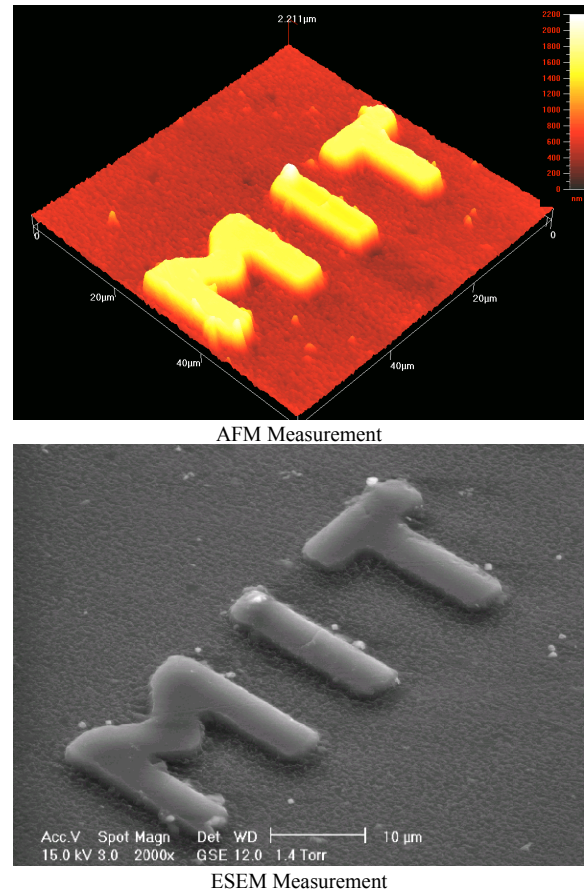


Figure 10 AFM and ESEM Images of a Scale 6 Part. Note the similarity in surface profiles, including the defect in at the top of the "I" (NB: the apparent convexity of the parts in the ESEM image is just that; other views show it to be very similar to the AFM image.)

artifacts were not mistaken as process variation. The AFM error had two components. The first was the machine resolution, which for most scans was ~0.04 μm . In addition, there was error associated with the interpretation of profiles like that shown in Fig. 11. To quantify the interpretation error, each measurement was re-interpreted 10 time, and from this an RMS error was determined (90% confidence t-distribution).



Figure 11 Width Profile for the "I" Feature from an AFM Scan. For this measurement the scan direction was actually along the long axis of the 'I', perpendicular to the width indicated.

Combining this with the resolution error yields an overall maximum RMS measurement error of 0.05 microns. The actual measurement data for the “worst” measurement is shown in Table 4

For the feature shown in Fig. 11, the corresponding run chart is shown in Fig. 12. The error bars indicate the maximum RMS measurement error. If we look at all the features captured by the AFM on the scale 6 feature a similar result is found. In Fig. 13 the deviation about the mean of 4 measurements is show along with the 0.05 micron error bars. Clearly there remains significant dimensional deviation regardless of the location of size of the feature.

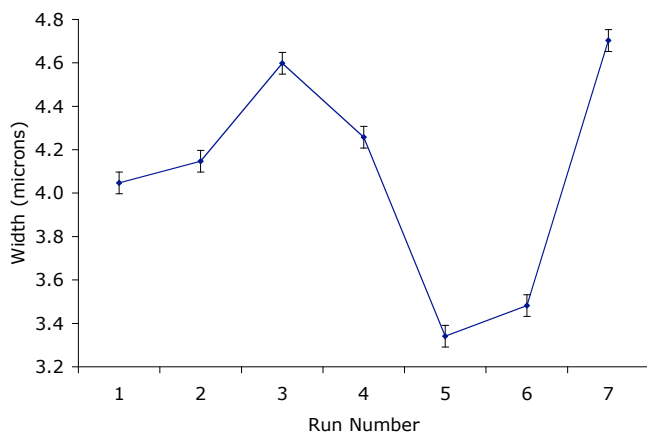


Figure 12 Run Chart Based on AFM Data for the “I” Width Measurement. Error bars of 0.05 microns are shown for the RMS measurement uncertainty.

TABLE 4
SUMMARY STATISTICS FOR FIG. 12 RUN CHART

Feature	Average Width (microns)	Standard Deviation (microns)	Coefficient of Variance (%)	Range (microns)	RMS Measurement error (microns)
Middle of the “I”	4.08	0.52	12.64	1.36	0.05

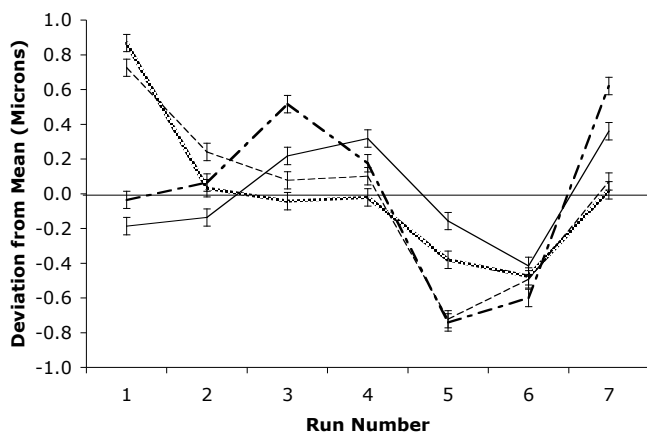


Fig 13 Width Deviation from Mean for All Scale 6 part measurements.

X. DISCUSSION

Measurements using the Zygo interferometer indicated a significant level of part-to-part dimensional variation (see Figs. 8 and 9) However, it was also found that the Zygo interferometer used for these measurements has a resolution that depended upon the range of view used. As shown in Table 3, this range was from 0.85 μm to 2.2 μm over the same scale as Fig. 9. Given that the resolution of the interferometer is on the same order of magnitude as the standard deviation, the data does not support any conclusions about inherent process variation.

However, when the smallest features were measured using AFM, it was unequivocal that significant process variation exists, and that it is at high levels that must be reduced. At this time the cause of such variation is not clear, and may have to do with the cycle to cycle variability of the machine, the uniformity of the thermal environment, or variability in the workpiece material.

XI. CONCLUSIONS

The explosion of interest in micro patterned polymers has been driven by numerous exciting applications in microfluidics, micro reactors and optics. While much has been done to establish the functional suitability of embossed product from PMMA and other materials, it is evident that the manufacturing implications of these methods have not received careful study. In this paper, we report preliminary experiments aimed at identifying the basic process variability of embossing at the micron scale. While the data proved hard to obtain, it was seen that considerable variation of basic dimensions exists. Based on this result we expect to conduct both fundamental polymer deformation studies to determine causes for such variation, and to explore means of reduction.

Obtaining robust process variation data require a both well-controlled equipment and consistent forming conditions. In addition, the part measurements must be of sufficient resolution to identify significant dimensional variation. In this study we have developed a lab scale embossing device that can provide a consistent thermal and mechanical environment for the embossing process. However, despite such controls, significant variation in the characteristic dimensions were observed, with a coefficient of variation as high as 13%. As micro-embossed parts transition to full-scale production such levels of variation will be unacceptable. Therefore, it is critical that the origins of this variation and means for its minimization be identified. Accordingly, our current work focused on both basic plastic flow modeling and improvement of the forming machine to permit large volumes of data to be obtained in minimal time. Finally, a new platen system is being developed that will greatly reduce the thermal cycle time, thereby introducing production rate maximization into the quality problem.

ACKNOWLEDGMENT

The authors gratefully acknowledge the Singapore MIT Alliance for support of this work.

REFERENCES

- [1] M. Krishnan, V. Namasivayam, R. Lin, R. Pal, and M. Burns, "Micro-fabricated reaction and separation systems," *Current Opinion in Biotechnology*, vol. 12, pp. 92-98, 2001.
- [2] A.J. Ricco, T. D. Boone, Z. H. Fan, I. Gibbons, T. Matray, S. Singh, H. Tan, T. Tian, and S. J. Williams, "Application of disposable plastic microfluidic device arrays with customized chemistries to multiplexed biochemical assays," *Biochemical Society Transactions*, vol. 30, part 2, 2002.
- [3] M. Pumera, J. Wang, H. Lowe, and S. Hardt, "Poly (methylmethacrylate) microchip electrophoresis device with thick-film amperometric detector: towards fully disposable lab-on-a-chip," presented at LabAutomation 2002, Palm Springs, CA.
- [4] T. Schulte, R. Bardell, B. Weigl, "Sample acquisition and control on-chip microfluidic sample preparation," *JALA*, vol. 5, no. 4.
- [5] L. J. Heyderman, H. Schiff, C. David, J. Gobrecht, and T. Schweizer, "Flow behavior of thin polymer films used for hot embossing lithography," *Microelectronic Engineering*, vol. 54, pp. 229-245, 2000.
- [6] H. Schiff, L. J. Heyderman, M. Auf der Maur, and J. Gobrecht, "Pattern formation in hot embossing of thin polymer films," *Institute of Physics Publishing, Nanotechnology*, vol. 12, pp. 173-177, 2001.
- [7] T. D. Boone, Z. H. Fan, H. H. Hooper, A. J. Ricco, H. Tan, S. J. Williams, "Plastic advances microfluidic devices," *Analytical Chemistry*, February 1, 2002.
- [8] Amic AB, "Biochips in plastics—future technology platforms for drug discovery," *Business Briefing, Pharmatech 2002*.
- [9] S.Y. Chou, P.R. Krauss and P.J. Renstron, "Imprint of sub-25 nm vias and trenches in polymers *Appl. Phys. Lett.*, Vol. 67, No. 21, 20 November 1995
- [10] D.E. Hardt, B. Ganesan, Q. Wang, M. Dirckx, and A. Rzepniewski, "Process Control in Micro-Embossing: A Review", *Proc. 4th Annual Symposium, Singapore, MIT Alliance, January, 2004*.
- [11] N. Roos, M. Wissen, T. Glinsner, H. C. Scheer, "Impact of vacuum environment on the hot embossing process," presented at SPIE's Microlithography, Santa Clara, CA, February 22-28, 2003.
- [12] N. Roos, T. Luxbacher, T. Glinsner, K. Pfeiffer, H. Schulz, and H. C. Scheer, "Nanoimprint lithography with a commercial 4 inch bond system for hot embossing," presented at SPIE's 26th Annual International Symposium Microlithography, Feb. 25 – March 2, 2001.
- [13] G. B. Lee, S. H. Chen, G. R. Huang, W. C. Sung, Y. H. Lin, "Microfabricated plastic chips by hot embossing methods and their applications for DNA separation and detection," *Sensors and Actuators B* 75, pp. 142-148, 2001.
- [14] Bacon, S. Tiwari and L. Rathbun, "Nanoimprinting by hot embossing in polymer substrates," *National Nanofabrication Users Network, Cornell Nanofabrication Facility*, pp. 6-7.
- [15] L. Lin, Y. T. Cheng, C. J. Chiu, "Comparative study of hot embossed micro structures fabricated by laboratory and commercial environments," *Microsystem Technologies*, vol. 4, pp. 113-116, 1998.
- [16] C-R. Lin, R-H. Chen, and C. Hung, "Preventing non-uniform shrinkage in open-die hot embossing of PMMA structures", *J. of Mat'ls Processing Technology*, vol. 140, 2003, pp. 173-179
- [17] B. Ganesan, "Process Control for Micro-Embossing: Initial Variability Study", *S.M. Thesis Mechanical Engineering, MIT, June, 2004*.